Chemical Engineering Journal 165 (2010) 370–377

Contents lists available at ScienceDirect

Chemical Engineering Journal

journal homepage: www.elsevier.com/locate/cej

Building block-tunable synthesis of self-assembled ZnO quasi-microspheres via a facile liquid process

Lanqin Tang[a,b], Shaofeng Yang[c], Yupeng Guo[b], Bing Zhou[b,*]

[a] College of Chemical and Biological Engineering, Yancheng Institute of Technology, 9 Yingbin Avenue, Yancheng 224051, PR China
[b] College of Chemistry, Jilin University, 2699 Qianjin Street, Changchun 130012, PR China
[c] Department of Chemical and Materials Engineering, University of Alberta, Edmonton, Alberta, T6G 2G6 Canada

ARTICLE INFO

Article history:
Received 13 July 2010
Received in revised form 1 September 2010
Accepted 3 September 2010

Keywords:
Self-assembled
ZnO
Microspheres
Building blocks

ABSTRACT

Self-assembled ZnO quasi-microspheres constructed of tunable building blocks have been grown directly through a facile liquid process. The effects of preparation parameters, such as the amounts of triethanolamine (TEA) and types of zinc counterions (SO_4^{2-}, CH_3COO^-), on the morphology of building blocks (BLs) have been examined. Experimental data show that TEA has played a dual key function in the self-assembly process; namely, one is to regulate the morphology of BLs, and the other is to induce the oriented attachment of these particles. A rational formation mechanism is proposed on the basis of detailed results of FESEM, TEM and zeta potentials tests. The overall formation of 3-D self-assembled ZnO quasi-microspheres can be summarized as: (a) growth of ZnO building blocks; (b) preassembly of these BLs into small aggregates; (c) further assembly of these aggregates to form special 3-D architectures. XRD and Raman spectra show that the self-assembled quasi-microspheres have wurtzite structures. Room-temperature PL spectra indicate that they have a potential application as ultraviolet emitters. This work presents a simple route using common organic molecules, TEA, as "growth modifiers", to the fabrication of novel 3-D self-assembled ZnO superstructures.

1. Introduction

Zinc oxide, as a versatile smart material, has unique applications in piezoelectric transducers and actuators [1], photovoltaic [2] and surface acoustic wave devices [3]. Particle size and morphology have a strong effect on their properties and applications [4–6]. Thus, various ZnO structures including nanobelts [7], nanoribbons [8], nanopins [9] and nanopellets [10] have been reported in the past few years.

Current interest in materials syntheses has focused on the use of nanoparticles as building blocks for the fabrication of 1-, 2- and 3-dimensional (D) superstructures [11–29]. And it is proved that special superstructures are an ideal host material for lasers, solar cells and other highly functional devices [30]. There are a number of methods available at the present time, which make use of various chemicophysical interactive forces among the building blocks (BLs) such as van der Waals interaction [12–15], chemical bindings [16–19], solvent adhesion and capillary action [20], hydrophilic and hydrophobic effects [21,22], electrostatic interactions [23] and magnetic attraction and repulsion [24–29]. Among these demonstrated methods, surfactant-assisted and solution-based self-assembly is a facile approach widely used in preparation of 1-, 2- and 3-D ZnO materials. However, compared with the great success in the spatial orientation of crystals, little attention has been devoted to the controlled organization of primary BLs into 3-D ZnO superstructures. Till now, there are few papers reported the fabrication of 3-D self-assembled ZnO structures through the polymeric surfactant-based way [30–33]. For example, Yu et al. reported the fabrications of 3-D microspheres composed of nanorods or nanosheets, which was achieved using two kinds of polymers, poly(sodium 4-styrenesulfonate) and poly(acrylic acid-co-maleic acid), respectively [30]. Zhang et al. realized the formation of 3-D ZnO microspheres through a water-soluble biopolymer (sodium alginate) assisted process at 100 °C for 7 h [32]. According to Zhao et al., by the calcinations of the precursor ($Zn_5(CO_3)_2(OH)_6$), which is obtained through a hydrothermal process with the assistance of $(PEO)_{20}$-$(PPO)_{70}(PEO)_{20}$ (P123), clew-like 3-D ZnO superstructures with nanosheets can be synthesized [33]. It seems that it is very necessary to introduce special polymers as the morphology modifiers and/or a further treatment of a precursor for the preparation of 3-D superstructures. Furthermore, fine control of 3-D structures is relatively difficult, which hinders the development of secondary organization of building blocks. From this point of view, it is strongly desirable to use common additives to the controllable construction of 3-D ZnO superstructures through a much simpler one-step approach.

* Corresponding author. Tel.: +86 431 8849 9134; fax: +86 431 8849 9134.
E-mail address: lanqin_tang@ycit.edu.cn (L. Tang).

1385-8947/$ – see front matter © 2010 Elsevier B.V. All rights reserved.
doi:10.1016/j.cej.2010.09.006

Table 1
Synthesis parameters of various ZnO samples.

Samples	Zn solution (1.0 M)	Theoretical Zn solution (mL)	Added Zn solution (mL)	TEA:Zn^{2+} (theoretical Zn)
A	$ZnSO_4$	50	50	1:3
A_1	$ZnSO_4$	50	18	1:3
A_2	$ZnSO_4$	50	30	1:3
C	$ZnSO_4$	50	50	1:1
D	$ZnSO_4$	50	50	2:1
A*	$Zn(CH_3COO)_2$	50	50	1:3

In this work, we report a solution-based one-step method to prepare 3-D ZnO self-assembled quasi-microspheres in the presence of common small-molecule triethanolamine (TEA). The morphology and size of BLs can be regulated only by changing the amount of TEA, which are of interest for various optoelectronic applications. In addition, the formation mechanism of the superstructures is discussed.

2. Experimental section

2.1. Materials

Zinc sulfate ($ZnSO_4$) was adopted as the source material for zinc species. Sodium hydroxide (NaOH) was employed as the precipitators for the formation of ZnO particles. Triethanolamine (TEA) was chosen as growth modifiers. All chemicals purchased from Beijing Chemicals Co. Ltd. were of analytical grade and used as received. Distilled water was used throughout.

2.2. Preparation of self-assembled ZnO quasi-microspheres

In a typical synthesis, 50 mL of a solution containing 0.1 mol of NaOH and a certain amount of triethanolamine (TEA) was prepared in a three-necked flask under stirring. Then 50 mL of 1.0 M $ZnSO_4$ solution was added dropwise to the flask at a rate of 1 mL/min at 70 °C, resulting in the formation of white precipitates. After the addition of $ZnSO_4$ solution, the obtained white precipitates were washed with distilled water and dried at 50 °C in air for 20 h. The molar ratio of TEA/$ZnSO_4$, R, was varied from 1:3 to 2:1. Experimental conditions for typical ZnO samples are listed in Table 1.

2.3. Characterization

The crystal structures of the products were examined by X-ray diffraction (XRD) with a D/max-RA Cu Kα diffractometer (λ = 0.154056 nm) employing a scanning rate of 0.02° S^{-1} in the 2θ ranges from 30 to 70°. The morphologies of the samples were studied by field emission scanning electron microscopy observations (FESEM, JEOL JSM-6700F) with an acceleration voltage of 5 kV, transmission electron microscopy (TEM, Hitachi H-8100) operated at 300 kV, and high resolution transmission electron microscopy (HRTEM, JEOL JEM-3010). The zeta potentials of the reaction system were analyzed by a Zeta Potential Analyzer (BI-ZetaPALS). Raman spectra were obtained on a Renishaw 1000 spectroscope (Ar ion laser, 514.5 nm). Room-temperature photoluminescence spectra (PL) were achieved on an Edinbergh instrument FLS 920 spectroscope using a 320 nm excitation line.

3. Results and discussion

3.1. Structural and morphological characteristics

The XRD pattern of sample-A is shown in Fig. 1b. All the diffraction peaks exhibit a wurtzite structure of ZnO with cell constants of $a = 0.325$ nm and $c = 0.521$ nm, which are consistent with the values shown in the standard card (JCPDS card No. 36-1451, Fig. 1a). The relative intensity of the (0 0 2) peak in Fig. 1b is slightly stronger than that of the (1 0 0) peak. This indicates that sample-A has a preferential orientation along the *c* axis [31]. Furthermore, the average crystal size of sample-A is 39 nm calculated from the broadening for each (1 0 1) diffraction peaks using Scherrer equation. The smaller its grain size, the higher its gas sensitivity is [34].

As shown in Fig. 2a, sample-A exhibits quasi-spherical morphology with an average diameter of about 10 μm. Most of the microspheres are formed by the gathering of small aggregates (Fig. 2b, indicated by circles). It is obvious that there are just disordered pores rather than ordered channels in our individual ZnO superstructures. High-magnification FESEM image in Fig. 2c shows that the surfaces of the microspheres are composed of a number of 1-D nanorods. The diameters of these nanorods range from 10 to 50 nm. The X-ray energy dispersive spectroscopy (EDS) result shown in Fig. 2d demonstrates that the as-prepared sample contains only Zn and O, and the atomic ratio of Zn and O is about 50.65:49.35.

The structure of the self-assembled spheres is further investigated by TEM. As an additional evidence to the directly assembly nature, ultrasonic treatment is applied to break the inter-rod linkage. From Fig. 3a, 1-D nanorods could be observed, which can provide much more effective surface area for absorption. Therefore, this unique self-assembled superstructure can be used in the photodecomposition of organic compounds and catalyst support [35]. The selective area electron diffraction (SAED) pattern taken from dot-circle indicated part is shown in the inset of Fig. 3a. Diffraction circles, which are composed of diffraction spots, can be indexed to the wurtzite structure with phase purity and the polycrystalline nature of the prepared ZnO superstructures. The high resolution transmission electron microscopy (HRTEM) image of a nanorod is demonstrated in Fig. 3b. The lattice space can be determined to be

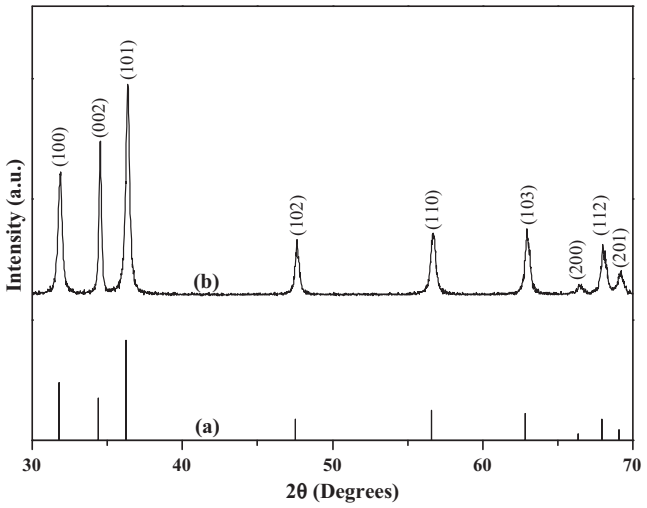

Fig. 1. Calculated X-ray diffraction pattern of ZnO (a) and the X-ray diffraction pattern of the as prepared sample-A (b).

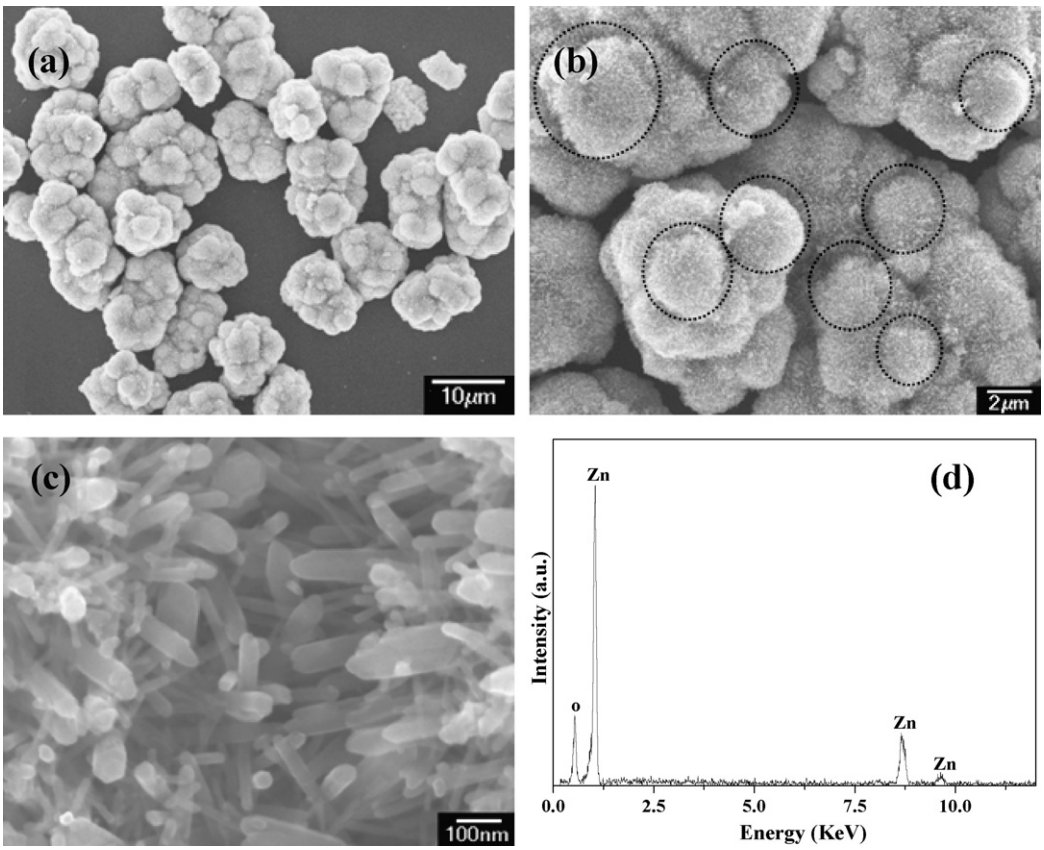

Fig. 2. Low-magnification FESEM image of large-scale self-assembled ZnO microspheres (sample-A) (a), enlarged FESEM image of ZnO crystals (b), nanorod-assembled surface FESEM image of ZnO microspheres (c) and EDS pattern of the ZnO microspheres (d).

0.26 nm, corresponding to the (0 0 2) plane of hexagonal ZnO. This suggests that the growth direction of the 1-D building blocks is the *c* axis ([0 0 1]).

3.2. Growth process

To examine the morphological evolution of the ZnO superstructures during the addition of $ZnSO_4$ solution, two samples named sample-A_1 and sample-A_2 are collected with the volumes of added $ZnSO_4$ solution being 18 mL and 30 mL, respectively. In the early stage of the addition of $ZnSO_4$ solution, no white precipitates are observed. When 18 mL of $ZnSO_4$ solution is added, a large amount of small aggregates is interestingly observed (sample-A_1, Fig. 4a). Three main diffraction peaks of it at 31.9, 34.54 and 36.36 are well indexed as the hexagonal phase of wurtzite ZnO (see the inset image of Fig. 4a), indicating the rapid characteristic of our synthesis method. The magnified FESEM image shown in Fig. 4b reveals that these aggregates made up of ZnO nanorods, have a small size range of 300–500 nm. When the volume of added $ZnSO_4$ solution is 30 mL, large superstructures composed of small aggregates are produced (sample-A_2, Fig. 4c), which is similar to sample-A shown in Fig. 2. Furthermore, the diameters of the superstructures are in the range of 1–6 μm. From the high-resolution FESEM image shown in Fig. 4d, the building blocks show nanorod-like morphology. To further get the information of the size and morphology of these two kinds of BLs, long-time ultrasonic treatment of about 20 min is also

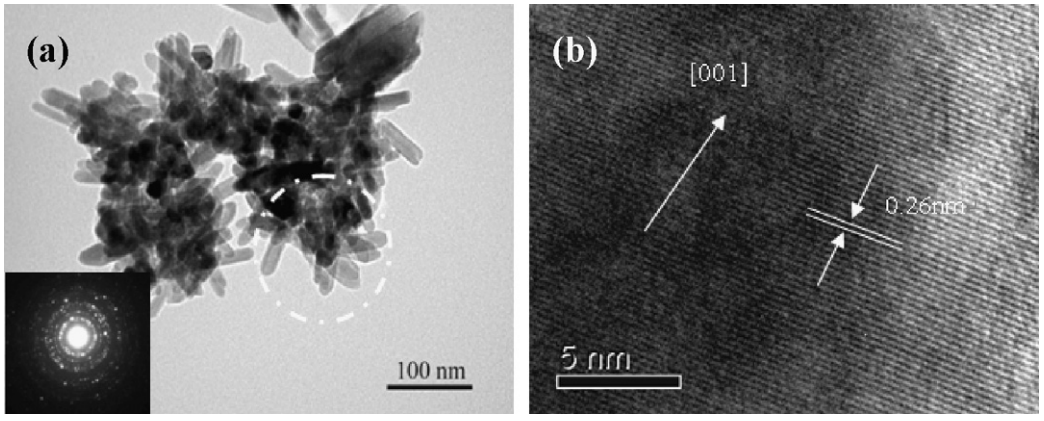

Fig. 3. TEM image of sample-A after being treated in an ultrasonic bath and the corresponding SAED pattern taken from dot-circle indicated part ((a) and the inset), and HRTEM image taken from the head part of one nanorod (b).

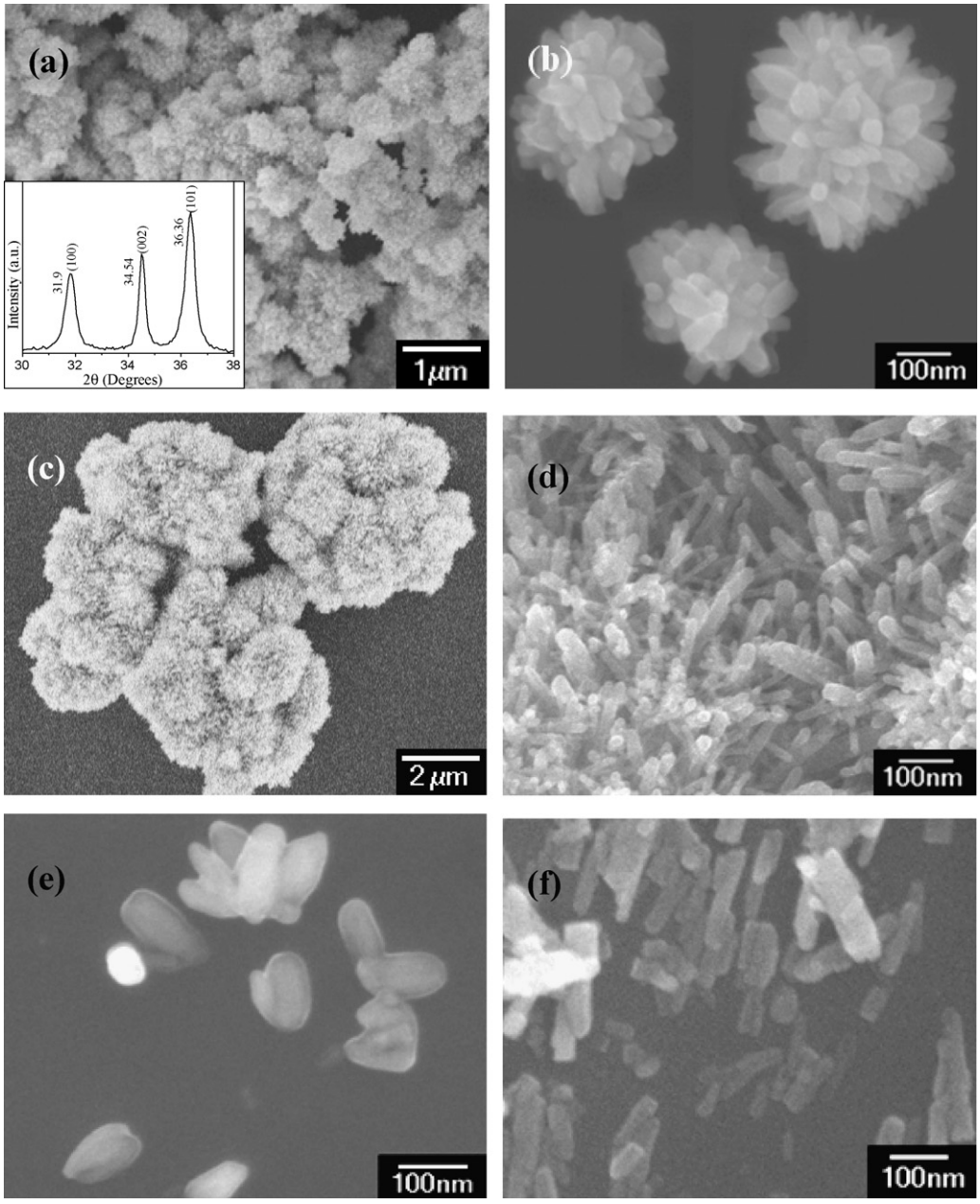

Fig. 4. Low-magnification and enlarged FESEM images of ZnO sample-A_1 (a and b) and -A_2 (c and d) obtained with the volumes of added $ZnSO_4$ solution being 18 mL and 30 mL, respectively, and FESEM images of building blocks of sample-A_1 (e) and -A_2 (f).

applied. After being treated in an ultrasonic bath, these rod-like BLs of sample-A_1 (Fig. 4e) and sample-A_2 (Fig. 4f) become highly dispersed and the average diameters of them are about 80 nm and 60 nm, respectively.

3.3. Mechanism

Controlling the size and morphology of self-assembled superstructures as well as the BLs is of great prospect, which will endow the self-assembled superstructures with particular properties. In this work, we realize the regulation of the morphologies of BLs only by changing the amount of TEA. For example, by increasing the amount of TEA (R = 1:1), superstructures with a size of about 5 μm are obtained (sample-C, Fig 5a and b). Furthermore, FESEM image in Fig. 5c shows that the BLs of sample-C are tapered nail-like particles. Further increasing the molar ratio of TEA/$ZnSO_4$ to 2:1, 3-D microspheres tend to be broken and the BLs transform into 3-D quasi-spheres (sample-D, Fig. 5a2 and b2). From the FESEM image shown in Fig. 5c2, the BLs of sample-D show quasi-hemispherical morphology. These results prove that the superstructures can be obtained in a wide TEA/Zn^{2+} molar ratio range (1:3–2:1), and the morphologies of BLs can be regulated only by changing the amounts of TEA.

The effects of zinc counterions on the morphology of BLs are also studied. Sample-A* was prepared instead with the molar ratio of TEA/$Zn(CH_3COO)_2$ being 1:3. From Fig. 6a, it shows that the size and morphology of sample-A* are nearly the same as those of sample-A. High-resolution FESEM image in Fig. 6b indicates that the nanorod-like BLs have an average diameter range of 20–40 nm, which is slightly smaller than that of sample-A. It indicates that the morphologies of self-assembled superstructures and building blocks are almost independent on the types of the counterions (CH_3COO^- and SO_4^{2-}), which are quite different from the results reported ever [37,38].

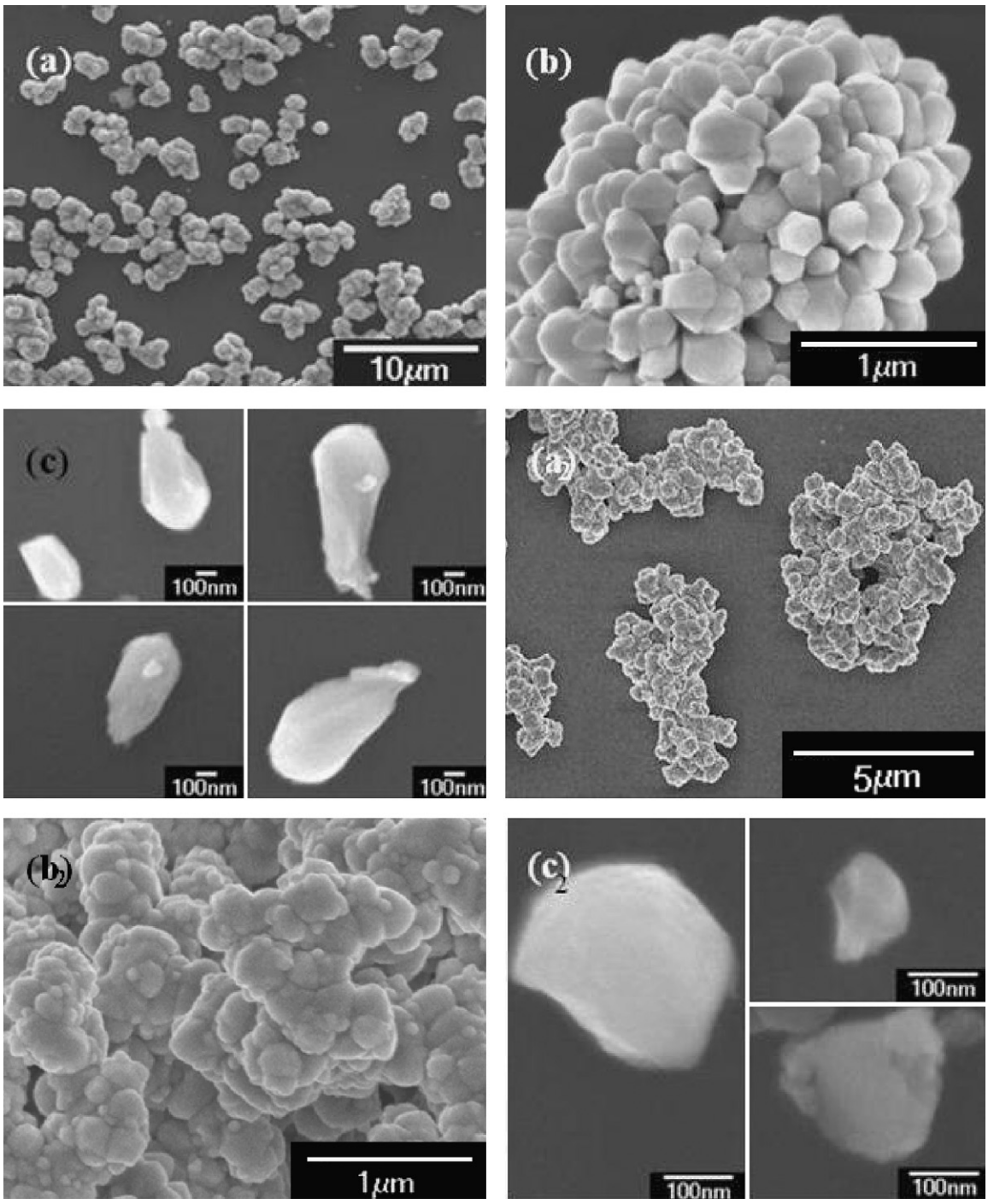

Fig. 5. Low-magnification and enlarged FESEM images of ZnO sample-C (a and b) and its corresponding FESEM images of building blocks (c), and low-magnification and enlarged FESEM images of ZnO sample-D (a_2 and b_2) and its corresponding FESEM images of building blocks (c_2).

In previous works, TEA usually acts as a complexing agent to produce ellipsoidal or spherical inorganic compounds [36,39,40]. For example, Yang and co-workers [36] have reported the synthesis of ellipsoidal ZnO particles by the hydrolysis of zinc acetate dihydrate in the presence of TEA by sonication. Jiang et al. [40] realized the fabrication of ZnO spheres using TEA aqueous solution as solvent and zinc nitrate hexhydrate as zinc source at reaction temperature ranging from 150 to 200 °C. These methods are based on masking Zn^{2+} ions with TEA first and then promoting the dissociation of the coordination complex to ZnO precipitates by sonication or higher temperature. But the controllable hierarchical organization of these particles has rarely been reported by the TEA-assistant solution process.

In our work, a new synthetic method is fabricated in order to produce self-assembled superstructures. Common TEA is specifically mixed with NaOH solution together first, so the protonation of it can be hampered [41]. Therefore, with the further addition of $ZnSO_4$ solution to above mixture, functional ZnO seeds (i.e. TEA adsorbed ZnO seeds) are formed. In order to explicate the importance of the functional ZnO seeds, two control experiments are conducted. When ZnO particles are fabricated by adding NaOH solution to the complex formed by $ZnSO_4$ solution and TEA (R = 1:3,

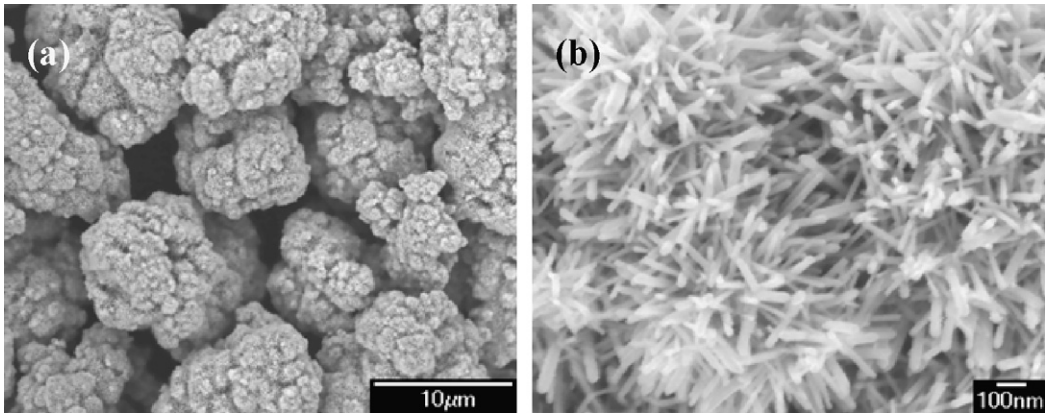

Fig. 6. Low-magnification (a) and enlarged (b) FESEM images of sample-A* obtained with the molar ratio of TEA/$Zn(CH_3COO)_2$ being 1/3.

70 °C), no superstructures composed of BLs but ZnO hexagonal slices with a side length of about 500 nm are obtained (Fig. 7a). Another ZnO sample is prepared in the absence of TEA. From the TEM image of this sample, only some nanoparticles are observed (Fig. 7b). Therefore, we believe that the formation of functional ZnO seeds in the alkaline solution make it possible to build self-assembled ZnO superstructures composed of BLs.

As for the formation mechanism of the special 3-D self-assembled ZnO superstructures, an "oriented attachment" may underlie the current synthesis [42]. At the early stage, functional ZnO seeds are generated with the addition of $ZnSO_4$ solution to the mixture solution formed by NaOH and TEA. The adsorption of TEA onto ZnO surfaces is convinced to follow the adsorption mechanism, from which each additive has its preferential adsorption face. Then primary ZnO seeds grow to distinct morphology due to the amounts of TEA (Figs. 2 and 5). In fact, selective adsorption of organic molecules to specific crystal surfaces leading to different morphologies has been extensively studied [43]. Like other amines, TEA acts as a weak base due to the lone pair of electrons on the nitrogen atom. So the adsorption of them, as well as NaOH, makes the surface of these primary ZnO particles negative, which is well consistent with the negative zeta potential data of the suspension (−8 mV). Therefore, free Zn^{2+} ions from the addition of $ZnSO_4$ solution, can spontaneously transfer onto the surfaces of ZnO particles by electrostatic actions, and grow into small aggregates. As the reaction further progresses, the small ZnO aggregates gradually gather together and finally evolve into spherical superstructures (Fig. 4). It is convinced that the driving force during such an aggregation process should be the reduction of surface free energy of the superstructure [33]. These results demonstrate a three-step process to form large 3-D self-assembled microspheres in the current reaction system: the growth of BLs, preassembly of the BLs into small aggregates, and subsequent assembly of these aggregates into quasi-microspherical superstructures.

3.4. Optical measurements

Raman and room-temperature PL spectra are carried out to evaluate the degree of crystallinity and the optical properties of the special 3-D self-assembled ZnO samples-A, -C and -D. The Raman spectra are shown in Fig. 8a. Among the detected peaks, the remarkable peak at 437 cm^{-1} belongs to the nonpolar optical phonon E_2 mode, which is corresponding to the band characteristic of wurtzite phase. The appearance of the longitudinal optical (E_1 LO, 581 cm^{-1}) mode is attributed to the formation of oxygen vacancies, or other defect states. The other two relatively high peaks at 331 and 379 cm^{-1} can be assigned to $3E_{2H}$–E_{2L} and A_{1T} modes. All of the observed Raman spectroscopic peaks indicate that the obtained 3-D self-assembled ZnO microspheres have wurtzite structures.

The PL properties of these 3-D self-assembled ZnO microspheres were examined with a He–Cd laser of 320 nm at room temperature. Emissions located in the blue and blue-green band (450, 466, 480, and 490 nm) exist for all the three samples (Fig. 8b). Besides, an ultraviolet (UV) emission band centering at about 360 nm is also detected. It is commonly accepted that the UV emission results from the annihilation of free excitons, while the emissions in the blue and blue-green band originate from electronic transitions from the ionized oxygen vacancies to the valence band, indicating structural

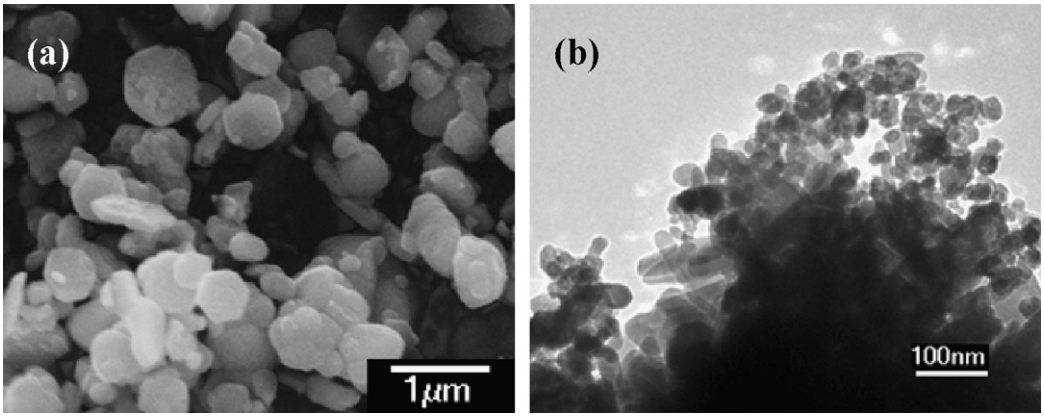

Fig. 7. FESEM image of ZnO particles fabricated by adding NaOH solution to the complex formed by $ZnSO_4$ solution and TEA (R = 1:3, 70 °C) (a), and TEM image of ZnO particles obtained in the absence of TEA (b).

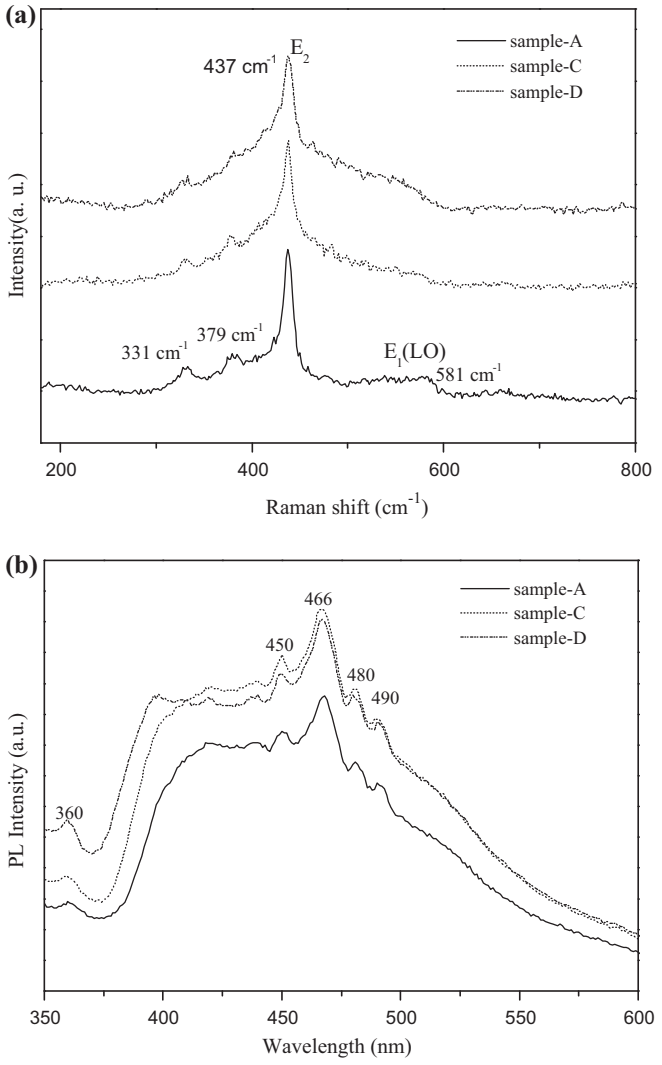

Fig. 8. Raman (a) and room-temperature PL (b) spectra of samples-A, -C and -D.

defects, such as oxygen vacancies and impurities, exist in these self-assembled superstructures. It shows that these materials can be potentially used as ultraviolet emitter.

4. Conclusions

In summary, we have demonstrated a novel TEA-oriented solution-based self-assembly approach to the fabrication of unique 3-D microspherical ZnO superstructures. Primary formation of functional ZnO seeds in the alkaline solution makes it possible to build self-assembled ZnO superstructures. TEA has dual functions in this self-assembly process: to regulate the morphologies of building blocks and control the oriented attachment of these nanoparticles. These findings demonstrate a convenient and simple technique for the production of self-assembled structures suitable for subsequent processing into devices. Raman and room-temperature PL measurements confirm the superior crystallinity and optical properties of ZnO superstructures. The prepared materials exhibit great potential in various practical applications, such as UV-light emitters, photocatalysts, solar cells, and gas sensors.

References

[1] E. Kayahan, White light luminescence from annealed thin ZnO deposited porous silicon, J. Lumin. 130 (2010) 1295–1299.
[2] X.H. Ju, W. Feng, X.Q. Zhang, V. Kittichungchit, T. Hori, H. Moritou, A. Fujii, M. Ozaki, Fabrication of organic photovoltaic cells with double-layer ZnO structure, Sol. Energy Mater. Sol. Cells 93 (2009) 1562–1567.
[3] Y.Q. Fu, J.K. Luo, X.Y. Du, A.J. Flewitt, Y. Li, G.H. Markx, A.J. Walton, W.I. Milne, Recent developments on ZnO films for acoustic wave based bio-sensing and microfluidic applications: a review, Sens. Actuators B 143 (2010) 606–619.
[4] A.V. Desai, M.A. Haque, Mechanical properties of ZnO nanowires, Sens. Actuators A 134 (2007) 169–176.
[5] V.I. Kushnirenko, I.V. Markevich, A.V. Rusavsky, Influence of boric acid as a flux on the properties of ZnO ceramics, Radiat. Meas. 45 (2010) 468–471.
[6] S. Baek, J. Song, S. Lim, Improvement of the optical properties of ZnO nanorods by Fe doping, Physica B 399 (2007) 101–104.
[7] R. Yousefi, B. Kamaluddin, Effect of S- and Sn-doping to the optical properties of ZnO nanobelts, Appl. Surf. Sci. 255 (2009) 9376–9380.
[8] J.G. Wen, J.Y. Lao, D.Z. Wang, T.M. Kyaw, Y.L. Foo, Z.F. Ren, Self-assembly of semiconducting oxide nanowires, nanorods, and nanoribbons, Chem. Phys. Lett. 372 (2003) 717–722.
[9] K. Hou, C. Li, W. Lei, X.B. Zhang, X.X. Yang, K. Qu, B.P. Wang, Z.W. Zhao, X.W. Sun, Influence of synthesis temperature on ZnO nanostructure morphologies and field emission properties, Physica E 41 (2009) 470–473.
[10] W.S. Chiu, P.S. Khiew, D. Isa, M. Cloke, S. Radiman, R. Abd-Shukor, M.H. Abdullah, N.M. Huang, Synthesis of two-dimensional ZnO nanopellets by pyrolysis of zinc oleate, Chem. Eng. J. 142 (2008) 337–343.
[11] P.X. Gao, Z.L. Wang, Mesoporous polyhedral cages and shells formed by textured self-assembly of ZnO nanocrystals, J. Am. Chem. Soc. 125 (2003) 11299–11305.
[12] Z.L. Wang, Z.R. Dai, S.H. Sun, Polyhedral shapes of cobalt nanocrystals and their effect on ordered nanocrystal assembly, Adv. Mater. 12 (2000) 1944–1946.
[13] V.F. Puntes, D. Zanchet, C.K. Erdonmez, A.P. Alivisatos, Synthesis of hcp-Co nanodisks, J. Am. Chem. Soc. 124 (2002) 12874–12880.
[14] F. Dumestre, B. Chaudret, C. Amiens, P. Renaud, P. Fejes, Super-lattices of bcc iron nanocubes synthesised from $Fe(N(SiMe_3)_2)_2$, Science 303 (2004) 821.
[15] J. Park, K. An, Y. Hwang, J.G. Park, H.J. Noh, J.Y. Kim, J.H. Park, N.M. Hwang, T. Hyeon, Ultra-large-scale syntheses of monodisperse nanocrystals, Nat. Mater. 3 (2004) 891–895.
[16] R.L. Penn, J.F. Banfield, Imperfect oriented attachment: a mechanism for dislocation generation in defect-free nanocrystals, Science 281 (1998) 969–971.
[17] D.S. Ginger, H. Zhang, C.A. Mirkin, The evolution of dip-pen nanolithography, Angew. Chem. Int. Ed. 43 (2004) 30–45.
[18] H.G. Yang, H.C. Zeng, Self-construction of hollow SnO_2 octahedra based on two-dimensional aggregation of nanocrystallites, Angew. Chem. Int. Ed. 43 (2004) 5930–5933.
[19] B. Liu, H.C. Zeng, Symmetric and asymmetric Ostwald ripening in fabrication of homogeneous core–shell semiconductors, Small 1 (2005) 566–571.
[20] J.X. Huang, A.R. Tao, S. Connor, R.R. He, P.D. Yang, A general method for assembling single colloidal particle lines, Nano Lett. 6 (2006) 524–529.
[21] A.D. Dinsmore, M.F. Hsu, M.G. Nikolaides, M. Marquez, A.R. Bausch, D.A. Weitz, Colloidosomes: self-assembled, selectively-permeable capsules composed of colloidal particles, Science 298 (2002) 1006.
[22] S. Park, J.H. Lim, S.W. Chung, C.A. Mirkin, Self-assembly of mesoscopic metal-polymer amphiphiles, Science 303 (2004) 348.
[23] E. Katz, I. Willner, Integrated nanoparticle-biomolecule hybrid systems: synthesis, properties and applications, Angew. Chem. Int. Ed. 43 (2004) 6042–6108.
[24] P.A. Smith, C.D. Nordquist, T.N. Jackson, T.S. Mayer, B.R. Martin, J. Mbindyo, T.E. Mallouk, Electric-field assisted assembly and alignment of metallic nanowires, Appl. Phys. Lett. 77 (2000) 1399–1401.
[25] V.F. Puntes, K.M. Krishnan, A.P. Alivisatos, Colloidal nanocrystal shape and size control: the case of cobalt, Science 291 (2001) 2115–2117.
[26] J.C. Love, A.R. Urbach, M.G. Prentiss, G.M. Whitesides, Three-dimensional self-assembly of metallic rods with sub-micron diameters using magnetic interactions, J. Am. Chem. Soc. 125 (2003) 12696–12697.
[27] D.L. Huber, Synthesis, properties and applications of iron nanoparticles, Small 1 (2005) 482–501.
[28] J.H Gao, B. Zhang, X.X. Zhang, B. Xu, Magnetic dipolar interaction induced self-assembly affords wires of cobalt selenide hollow nanocrystals, Angew. Chem. Int. Ed. 45 (2006) 1220–1223.
[29] H.M. Chen, R.S. Liu, H.L. Li, H.C. Zeng, Generating isotropic superparamagnetic interconnectivity for the two-dimensional organization of nanostructured building blocks, Angew. Chem. Int. Ed. 45 (2006) 2713–2717.
[30] J.C. Mo, M. Yu, L. Zhang, S.K. Li, Self-assembly of ZnO nanorods and nanosheets into hollow microhemispheres and microspheres, Adv. Mater. 17 (2005) 756–760.
[31] J.P. Liu, X.T. Huang, K.M. Sulieman, F.L. Sun, X. He, Solution-based growth optical properties of self-assembled monocrystalline ZnO ellipsoids, J. Phys. Chem. B 110 (2006) 10612–10618.
[32] S.Y. Gao, H.J. Zhang, X.M. Wang, R.P. Deng, D.H. Sun, G.L. Zheng, ZnO-based hollow microspheres: biopolymer-assisted assemblies from ZnO nanorods, J. Phys. Chem. B 110 (2006) 15847–15852.
[33] P. Bai, P.P. Wu, Z.F. Yan, J.K. Zhou, X.S. Zhao, Self assembly of clew-like ZnO superstructures in the presence of copolymer, J. Phys. Chem. C 111 (2007) 9729–9733.
[34] J.Q. Xu, Q.Y. Pan, Y.A. Shun, Z.Z. Tian, Grain size control and gas sensing properties of ZnO gas sensor, Sens. Actuators B 66 (2000) 277–279.

[35] B.B. Lakshmi, C.J. Patrissi, C.R. Martin, Sol–gel template synthesis of semiconductor oxide micro and nanostructures, Chem. Mater. 9 (1997) 2544–2550.
[36] R. Xie, D. Li, H. Zhang, D. Yang, M. Jiang, T. Sekiguchi, B. Liu, Y. Bando, Low-temperature growth of uniform ZnO particles with controllable ellipsoidal morphologies and characteristic luminescence patterns, J. Phys. Chem. B. 10 (2006) 19147–19153.
[37] M. Andrés Vergés, A. Mifsud, C.J. Serna, Formation of rod-like zinc oxide microcrystals in homogeneous solutions, Chem. Soc. Faraday Trans. 86 (1990) 959–963.
[38] R.A. McBride, J.M. Kelly, D.E. McCormack, Growth of well-defined ZnO microparticles by hydroxide ion hydrolysis of zinc salts, J. Mater. Chem. 13 (2003) 1196–1201.
[39] T. Trindade, J.D. Pedrosa de Jesus, P. O'Brien, Preparation of zinc oxide and zinc sulfide powders by controlled precipitation from aqueous solution, J. Mater. Chem. 4 (1994) 1611–1617.
[40] H. Jiang, J. Hu, F. Gu, C. Li, Large-scaled, uniform, monodispersed ZnO colloidal microspheres, J. Phys. Chem. C. 112 (2008) 12138–12141.
[41] J.L. Wyman, S. Kizilel, R. Skarbek, X.Y. Zhao, M. Connors, W.S. Dillmore, W.L. Murphy, M. Mrksich, S.R. Nagel, M.R. Garfinkel, Immunoisolating pancreatic islets by encapsulation with selective withdrawal, Small 3 (2007) 683–690.
[42] E.J.H. Lee, C. Ribeiro, E. Longo, E.R. Leite, Oriented attachment: an effective mechanism in the formation of anisotropic nanocrystals, J. Phys. Chem. B 109 (2005) 20842–20846.
[43] X.G. Peng, Mechanisms for the shape control and shape evolution of colloidal semiconductor nanocrystals, Adv. Mater. 15 (2003) 459–463.